Investigation of Relaxation Phenomena using 15MHz Pulsed Nuclear Magnetic Resonance

University of Cambridge, HoC: Professor Siân E Dutton

Experiment Completed: 17th - 30th October 2024

Abstract

The investigation of relaxation times in nuclear magnetic resonance (NMR) spectroscopy is the main focus of this experiment. The effects on the spin-lattice and spin-spin relaxation times due to changes in temperature and viscosity, and the addition of paramagnetic ions are investigated. It is found that the relaxation time is inversely proportional to the viscosity of the sample. Additionally, the addition of paramagnetic ions in the form of copper sulphate reduces the relaxation times, as paramagnetic ions allow for more efficient dipole-dipole relaxation mechanisms to occur. Increasing the temperature of viscous samples increases their decay time by reducing their viscosity and has no effect on samples affected by paramagnetic ions. A further experiment is also undertaken where the fluorine NMR spectroscopy of two unknown chemicals is measured and used to identify them.

Contents

1 Introduction

Nuclear magnetic resonance (NMR) is a technique whose discovery by Isidor Rabi[1] won the 1944 Nobel Prize in Physics. It is used extensively in medicine as MRI (magnetic resonance imaging) for diagnosis and research. Additionally, it is used in biochemistry and organic chemistry for analysis of chemicals. NMR is a phenomenon where nuclei that are acted on by an oscillating magnetic field produce electromagnetic signals that can be used to characterise the nucleus.

This experiment focuses on the phenomenon of relaxation. Specifically, it looks at how the spin-lattice and spin-spin relaxation times are affected by viscosity, temperature, and the addition of paramagnetic ions. In 1948, Nicolaas Bloembergen[2] found that the viscosity of a sample is inversely related to its spin-lattice relaxation time. This experiment attempts to verify that theory. The experiment also attempts to demonstrate that the addition of paramagnetic ions to a sample reduces its relaxation time.

2 Theory

2.1 Angular Momentum and Spin

The magnetic nuclei at the centre of many atoms possess a property known as *spin*, which is an intrinsic form of angular momentum. Hydrogen and fluorine are the focus of this experiment which have spin: $s = \frac{1}{2}$. The spin angular momentum is given by $\boldsymbol{J} = m_s\hbar$ (where $m_s = \pm\frac{1}{2}$).[3]

The magnetic moment of a nucleus is given by $\boldsymbol{\mu} = \gamma\boldsymbol{J}$ where γ is the gyromagnetic ratio of the nucleus. When this nucleus is placed into an external magnetic field $\boldsymbol{B}$ its magnetic energy changes by $E = -\boldsymbol{\mu}\cdot\boldsymbol{B}$ and in the presence of a strong field, the spin axis (z) coincides with the field direction, giving equation 1.[3]

$$E = -\boldsymbol{\mu}\cdot\boldsymbol{B} = -\mu_z B_0 = -\gamma\hbar m_s B_0 \tag{1}$$

Since $m_s = \pm\frac{1}{2}$ the energy levels in the nuclei of fluorine and hydrogen are separated by $\hbar\gamma B_0$ which gives the resonance condition for NMR spectroscopy: the change in energy level $\Delta E = \hbar\gamma B_0$. Since $E = h\nu$ the resonance frequency can be determined (equation 2).[3]

$$\nu_0 = \frac{|\gamma|B_0}{2\pi} \tag{2}$$

2.2 Nuclear Magnetic Resonance Spectroscopy

NMR spectroscopy itself involves the following stages. Firstly, a magnetic field, B_0, is applied to a sample, generating two distinct energy levels in the sample as spins align with and against the field. Next, an oscillating pulse referred to as the RF (radio frequency) pulse is applied at the resonant frequency, which excites some lower energy nuclei to the higher state. As the sample relaxes (see section 2.3) to equilibrium, it emits electromagnetic waves, which can be analysed to give information on the sample (see section 2.5).

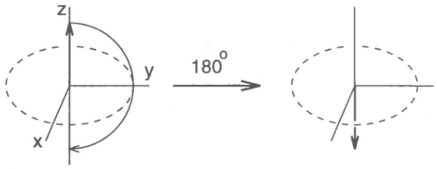

Figure 1: 180° Pulse[6]

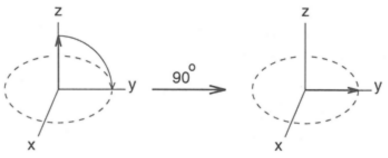

Figure 2: 90° Pulse[6]

2.3 Relaxation

Spin-Lattice Relaxation. When the RF pulses are applied to the sample in NMR spectroscopy, the magnetic vector moves away from the z axis (aligned with B_0) and into the x-y plane. After the pulses are removed the sample relaxes back to its equilibrium state. This relaxation is spin-lattice relaxation and is characterised by the decay time T_1 as seen in equation 3 where $M_z(t)$ is the magnitude of the z-magnetisation and M_z^{eq} is the value of M_z at equilibrium.[4] The relaxation occurs by the loss of energy from the excited spins to the molecular lattice, hence the name spin-lattice relaxation.[5]

$$\frac{dM_z(t)}{dt} = -\frac{M_z(t) - M_z^{eq}}{T_1} \tag{3}$$

This equation can be integrated to give equation 4 where $M_z^0 = M_z(t = 0)$

$$M_z(t) = (M_z^0 - M_z^{eq})e^{-\frac{t}{T_1}} + M_z^{eq} \tag{4}$$

Spin-Spin Relaxation. The second process of relaxation arises since the different spins in the sample exchange energy with each other. This means that some now precess faster or slower, resulting in a fanning out of spins in the xy plane. Overall, this leads to a detectable signal that is governed by the characteristic decay constant T_2. The process is described by equation 5 which similarly can be integrated to give equation 6.

$$\frac{dM_{xy}}{dt} = -\frac{M_{xy}}{T_2} \tag{5}$$

$$M_{xy}(t) = M_{xy}^0 e^{-\frac{t}{T_2}} \tag{6}$$

The Dipole-Dipole Relaxation Mechanism The dipole-dipole relaxation mechanism is a very efficient relaxation mechanism that only occurs in the presence of another particle possessing spin. In dipole-dipole relaxation, the nucleus experiences a small field due to the dipolar interaction; fluctuations in this field allow for a quicker relaxation mechanism. The presence of dissolved paramagnetic ions (such as $CuSO_{4(aq)}$) enables dipole-dipole relaxation. This is because the gyromagnetic ratio of the electron is around 657 times that of the proton.[5] This effect is utilised in NMR by adding paramagnetic ions to samples with long relaxation times.[5]

2.4 180° and 90° pulses

In order to measure the relaxation times, pulses are applied to the sample to move the magnetisation away from equilibrium. This experiment uses two forms of pulse, 90° and

180° pulses. A 90° pulse moves the M_z vector into the x-y plane, and a 180° pulse flips the vector into the negative z direction. These are illustrated in figures 1 and 2.

2.5 Spectroscopy

One of the most prevalent uses of NMR is NMR spectroscopy, which is used to identify the composition of chemical samples. The magnetic field applied to samples in NMR induces orbital electrons to circulate, which generates a *shielding* magnetic field. Chemical shifts arise due to this phenomenon. The actual field experienced by the nucleus is given by equation 7, where σ is the shielding constant.

$$B = B_0(1 - \sigma) \tag{7}$$

As a result of this equation 2 becomes equation 8

$$\nu_0 = \frac{|\gamma|B_0}{2\pi}(1 - \sigma) \tag{8}$$

The chemical shift can be defined using the shielding constant, but this is inconvenient. Instead, since absolute shifts are rarely needed, chemical shifts are defined in reference to some *reference nucleus* in equation 9.

$$\delta = 10^6 \left(\frac{\nu_0 - \nu_{0,\text{ref}}}{\nu_{\text{spec}}} \right) \tag{9}$$

In this equation $\nu_{0,\text{ref}}$ is the resonant frequency of the reference sample, and ν_{spec} is the spectrometer frequency. The result is multiplied by 10^6 to scale the shifts to a more convenient size; δ values are quoted in ppm (parts per million).

2.6 Determining the Viscosity of a Mixture

Part of this experiment explores the relationship between the relaxation times of glycerol with its viscosity. The viscosity is changed by using various concentrations of glycerol. To determine the viscosity of concentrations less than 100% the Gambill[7] approximation model is used (equation 10). Table 1 gives some example values.

$$\nu_{\text{mix}}^{\frac{1}{3}} = x_a \nu_a^{\frac{1}{3}} + x_b \nu_b^{\frac{1}{3}} \tag{10}$$

Viscosity	**Glycerol Concentration**
1412 mPa·s	100%
865.8 mPa·s	80%
454.7 mPa·s	60%
182.5 mPa·s	40%
41.19 mPa·s	20%
1 mPa·s	0%

Table 1: Viscosities of given concentrations (by volume) of Glycerol calculated using the Gambill method[7]

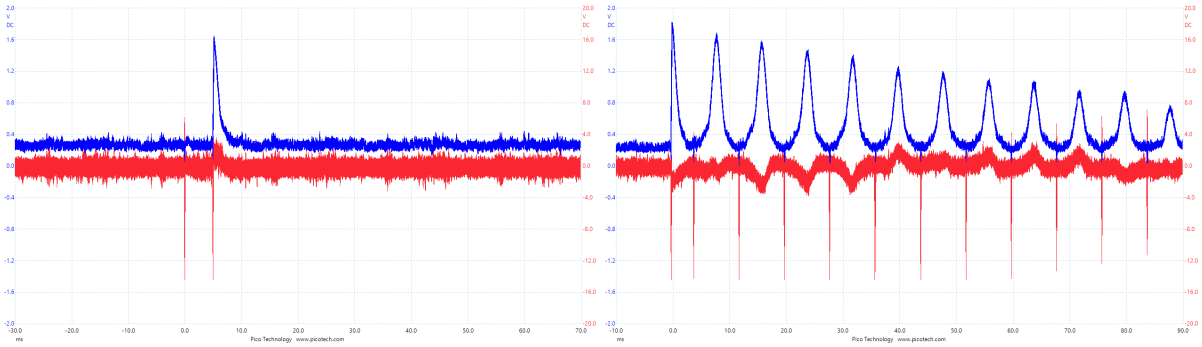

(a) T_1 (b) T_2

Figure 3: Example picoscope readings for T_1 and T_2 measurements using a 50 µL sample of 80% concentration blue. The blue trace is the *Detector Out* output, and the blue trace is the *Mixer Out* output.

3 Method

The instrumentation used in this experiment is the PS1/A pulsed NMR spectrometer (see appendix for block diagram). In figure 3 the blue trace is the *Detector Out* output, proportional to the peak amplitude of the receiver coil, and the red trace is the *Mixer Out* output, proportional to the frequency difference between the RF pulses and the sample's magnetisation. The condition for resonance is that zero beats occur in the red pulse, indicating the RF and sample frequencies are matched. The zero level of the trace (found using built-in picoscope analysis) was usually not zero and was therefore subtracted from all readings taken.

3.1 Preliminary Experiments

3.1.1 Choice of Sample Size

Samples of 50 µL were used in this experiment. Smaller samples are expected to yield weaker NMR signals, and larger samples are expected to be more affected by any inhomogeneities in the B-field. To test this theory, different sample sizes of $CuSO_4$ and glycerol were analysed (see figure 4). Small samples had very shallow peaks, making them hard to measure. No correlation between sample size and relaxation times was found, suggesting larger samples were not affected by field inhomogeneities; however, it could be that the samples tested were not large enough to detect these effects.

3.1.2 Magnetic Sweet Spot

It is essential to ensure the sample is placed in a uniform magnetic field to avoid any errors from field variations. To find the ideal positioning of the magnet, a 90° pulse was applied to a 100 µL glycerol sample, and the x and y positions of the sample were varied to produce figure 5. The peak magnetisation follows a quadratic function in x and y. The position of minimum variation was therefore determined to be at $x = 0$ and $y = 7$.

3.1.3 Off Resonance Behaviour

Figure 6 demonstrates the effect of not having the system at the resonance when measuring the peak magnetisation. A 90° pulse was applied to an 80% glycerol sample at

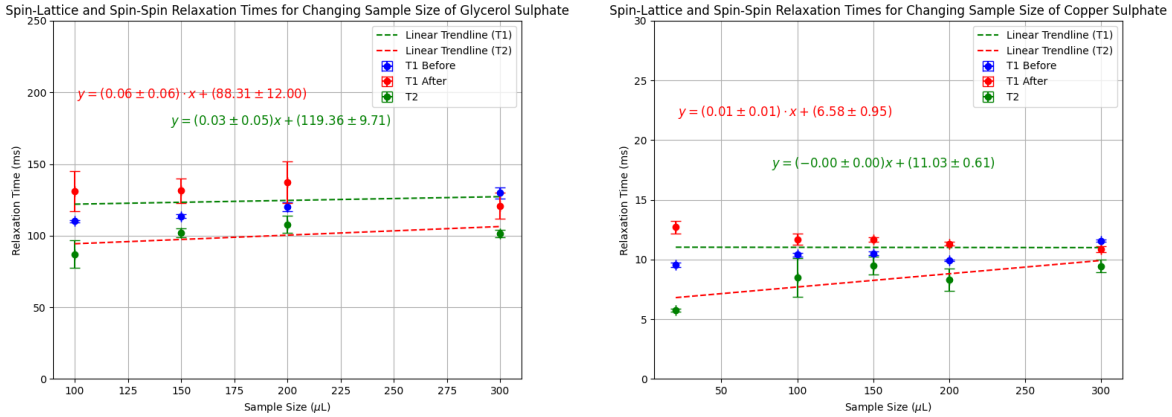

(a) Glycerol (b) $CuSO_4$

Figure 4: Plots of the Spin-Lattice (green line) and Spin-Spin (red line) relaxation times for varying sample sizes of 6.25% copper sulphate and 80% glycerol. No clear trend is seen between the sample size and relaxation times.

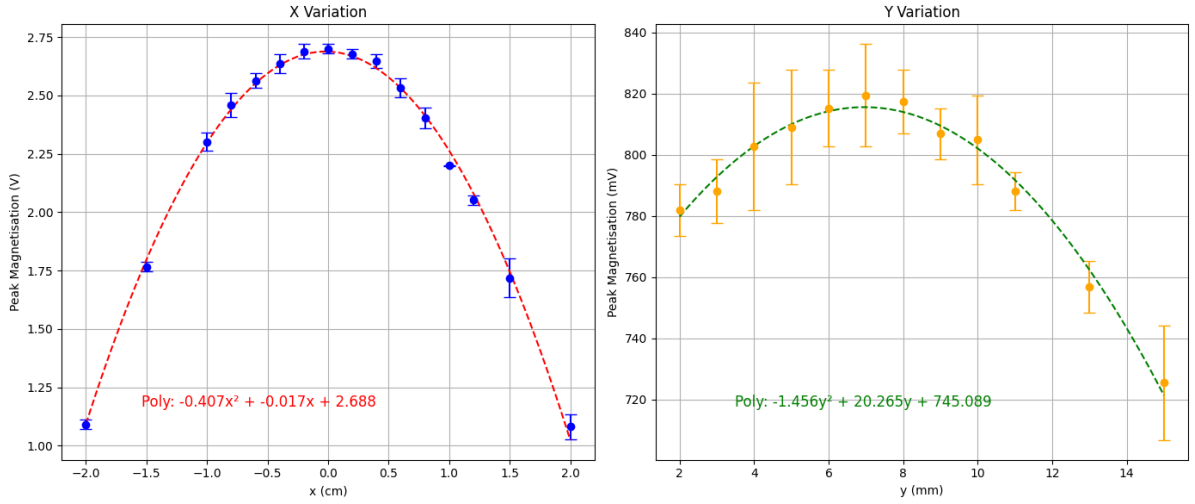

Figure 5: Measurement of the variation in the peak magnetisation with x and y positioning in the magnet. The *sweet spot* of the magnet was found to be at $x = 0$ and $y = 7$.

room temperature, and the peak magnetisation was measured. It is clear that as the frequency drifts away from the peak frequency ($\sim$ 15.618MHz) the 90° pulse are no longer perfect 90° pulses as the peak decreases. Subsidiary maxima are seen on either side of the resonance corresponding to a weaker 90° pulse.

3.2 Relaxation Experiments

The main bulk of the experimentation was the investigation of the effects of concentration and temperature on the relaxation times of glycerol and $CuSO_4$. 100% concentration samples of glycerol and $CuSO_4$ were mixed with various amounts of deionised water to produce samples of various concentrations. A water bath with a thermometer was used to heat up samples to specific temperatures. For temperatures below room temperature, an ice bath was used.

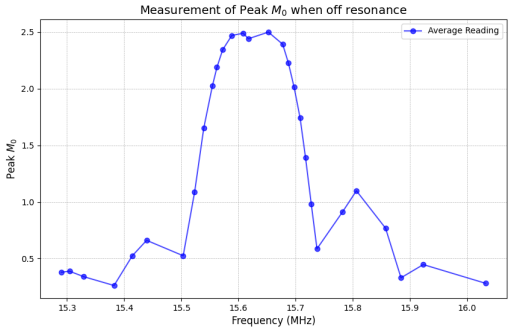

Figure 6: Measurement of the peak magnetisation of a 90° pulse with varying frequency of an 80% glycerol sample at 21°C. The peak magnetisation diverges from it's maximum when the frequency is away from resonance, and the 90° or 180° pulses are not complete pulses. Hence, experiments should be performed at resonance for the most accurate results.

3.2.1 Measuring Spin-Lattice Relaxation Time (Inversion Recovery)

The equilibrium magnetisation value was measured by applying a 90° pulse to the sample and measuring the resulting peak magnetisation. This pulse was then removed and replaced with a 180° pulse (pulse A) followed by a 90° pulse (pulse B) a time τ after. The peak magnetisation of pulse B was recorded. The 90° pulse is required to bring the spin into the measurable x-y plane; 90° pulses are applied at different times to view M_z at that time. The relaxation time is governed by equation 3, and since M_z is initially flipped with a 180° pulse, $M_z^0 = -M_z^{eq}$, equation 4 is rewritten as equation 11. Plotting a graph of $\ln \frac{M_z^{eq}-M_z}{2M_z^{eq}}$ against the delay time gives a linear graph with a gradient equal to $-\frac{1}{T_1}$ (see appendix), hence, T_1 can be determined by taking the reciprocal of the gradient.

$$M_z(t) = M_z^{eq}(1 - 2e^{-\frac{t}{T_1}}) \tag{11}$$

In taking these measurements, there were errors in the measured values of the peaks of M_z and M_z^{eq}. The error in $\ln \frac{M_z^{eq}-M_z}{2M_z^{eq}}$ was determined using equation 12[†].

$$\Delta \ln \frac{M_z^{eq} - M_z}{2M_z^{eq}} = \sqrt{\left(\frac{\Delta M_z}{M_z^{eq} - M_z}\right)^2 + \left(\frac{M_z \Delta M_z^{eq}}{M_z^{eq}(M_z^{eq} - M_z)}\right)^2} \tag{12}$$

3.2.2 Measuring Spin-Spin Lattice Relaxation Time

For measurement of the spin-spin lattice relaxation time, a 90° pulse is applied (pulse A), the magnitude of this is measured to give the equilibrium magnetisation as before. Then a 180° pulse (pulse B) is applied after a time τ and an echo is observed after a time 2τ. Successive pulses are then applied, and the amplitudes of the decaying spin echoes are recorded. The relaxation time is governed by equation 5. Plotting a graph of $\ln \frac{M_x y}{M_x y^0}$ against the delay time gives a graph with gradient $-\frac{1}{T_2}$ (see appendix) and hence T_2 can be found by taking the reciprocal of the gradient. As before there were errors in M_z and M_z^{eq} and the error in $\ln \frac{M_x y}{M_x y^0}$ are determined using equation 13.

[†]This and equation 13 were determined using the following equation for error propagation: $(\Delta X)^2 = \sum_{i=0}^{n} (\frac{\delta X}{\delta x_i} \Delta x_i)^2$ where $X = f(x_0, x_1, x_2, ..., x_n)$.

$$\Delta \ln \frac{M_z}{M_z^{eq}} = \sqrt{\left(\frac{\Delta M_z}{M_z}\right)^2 + \left(\frac{\Delta M_z^{eq}}{M_z^{eq}}\right)^2} \tag{13}$$

3.3 Analysing Data

For these experiments, the data was plotted in Python using the errors as explained above (example plots can be found in the appendix, figure 15). The error in the concentration and delay time were found to be negligible compared to the error in magnetisation. The error in the gradients was found by calculating the steepest and shallowest gradients within error. The T_1 and T_2 values generated from this were then plotted against concentration, viscosity, or temperature to view the trends in the data. The gradients in the trends were found using linear regression from the Python package *scipy.optimize.curve_fit*.

4 Results

4.1 Varying Concentration of Copper Sulphate

Glycerol			**Copper Sulphate**		
Viscosity/mPa·s	T_1/ms	T_2/ms	**Concentration/%**	T_1/ms	T_2/ms
1122	65.7±2.0	41.3±5.7	12.5	6.36±0.47	4.36±0.34
865.8	111.1±2.3	85.0±3.9	6.25	9.81±0.91	6.1±1.2
454.7	215.6±9.5	192±28	3.125	25.2±1.4	18.3±5.2
301.4	709±17	116±47	1.5625	51.3±1.5	26±12

Table 2: Example T_1 and T_2 values for different viscosities and concentrations of glycerol and copper sulphate. Relaxation times increase with reducing viscosity/concentration.

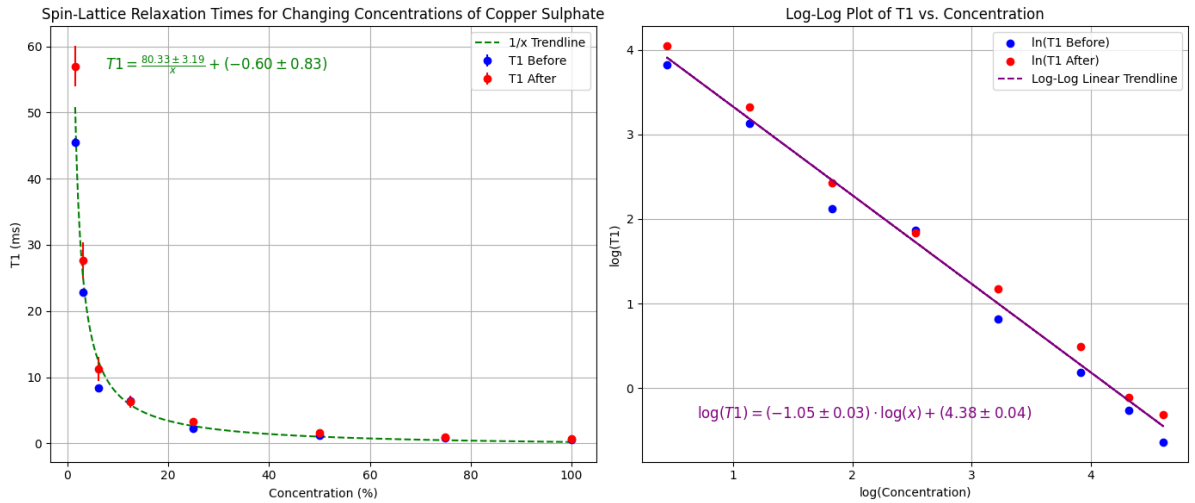

Figure 7: Plot of Spin-Lattice Relaxation time for different concentrations of copper sulphate at 21°C. An inverse relationship between T_1 and concentration is found.

In figure 7 the spin-lattice relaxation time (T_1) of $CuSO_4$ is plotted for varying concentrations. Additionally, $\ln T_1$ is plotted against ln(concentration). The gradient of this

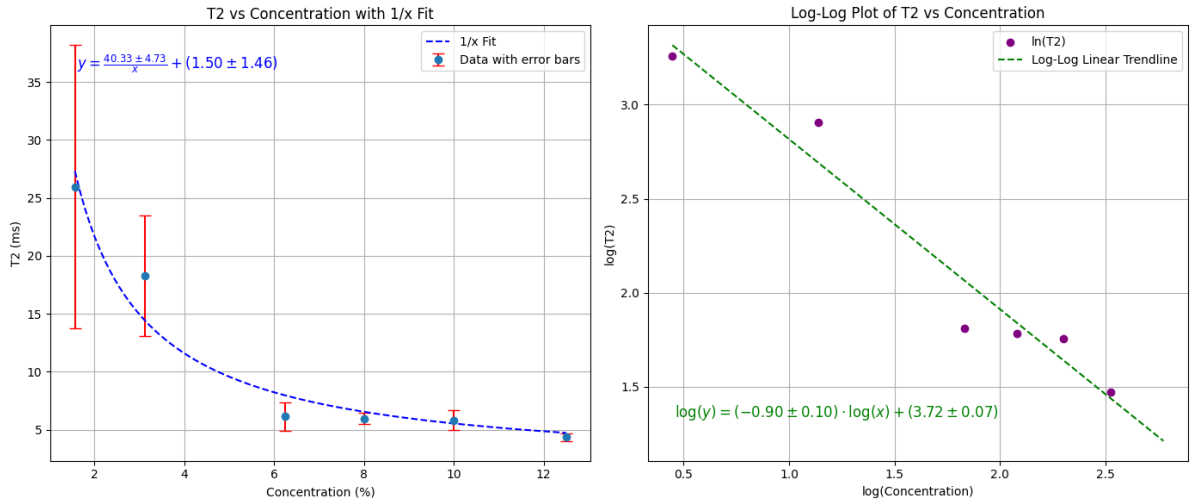

Figure 8: Plot of Spin-Spin Relaxation time for different concentrations of copper sulphate at 21°C. An inverse relationship between T_2 and concentration is found.

is found to be -1.05±0.03, implying an inverse relationship between T_1 and concentration. Similar trends are seen in figure 8, the gradient of the log-log graph is found to be -0.9±0.1, showing that T_2 is also inversely related to concentration.

An important thing to note is that for all T_1 graphs (see appendix figure 15) across $CuSO_4$ and glycerol, the T_1 value changes when M_z reaches zero. This is the origin of the before and after T_1 values on the graphs and is discussed in more detail in section 5.1.1.

4.2 Varying Viscosity of Glycerol

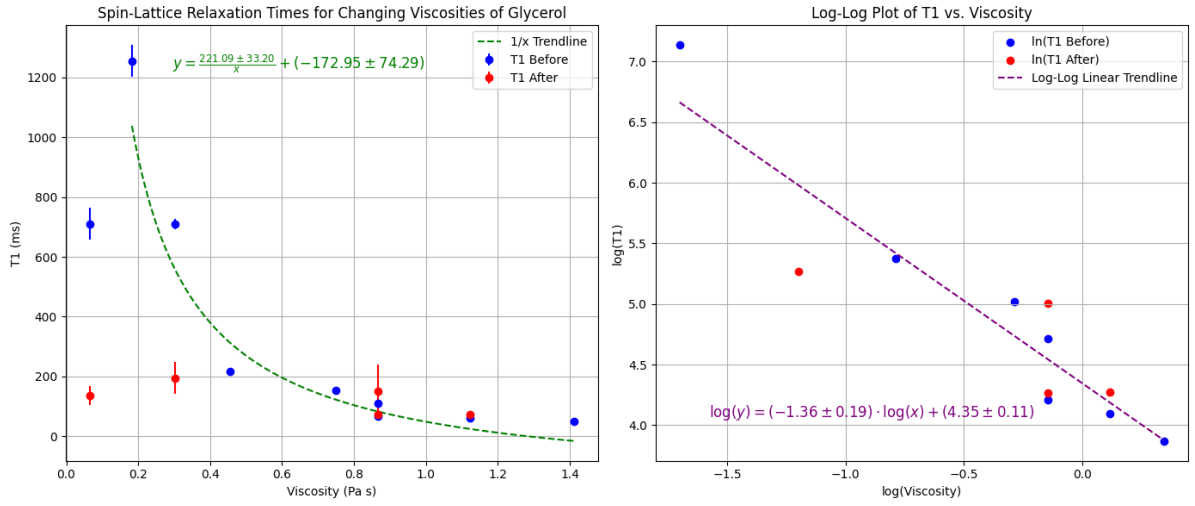

Figure 9: Plot of Spin-Lattice Relaxation time for different viscosities of glycerol at 21°C. An inverse relationship between T_1 and viscosity is found.

The resulting trends for this experiment (see figures 9 and 10) are similar to the $CuSO_4$ concentration experiment. There is noticeably more variation in the results for this experiment, however, especially for T_1. Anomalous points on these graphs were not included when running the regression method but are shown on the graph. The gradients

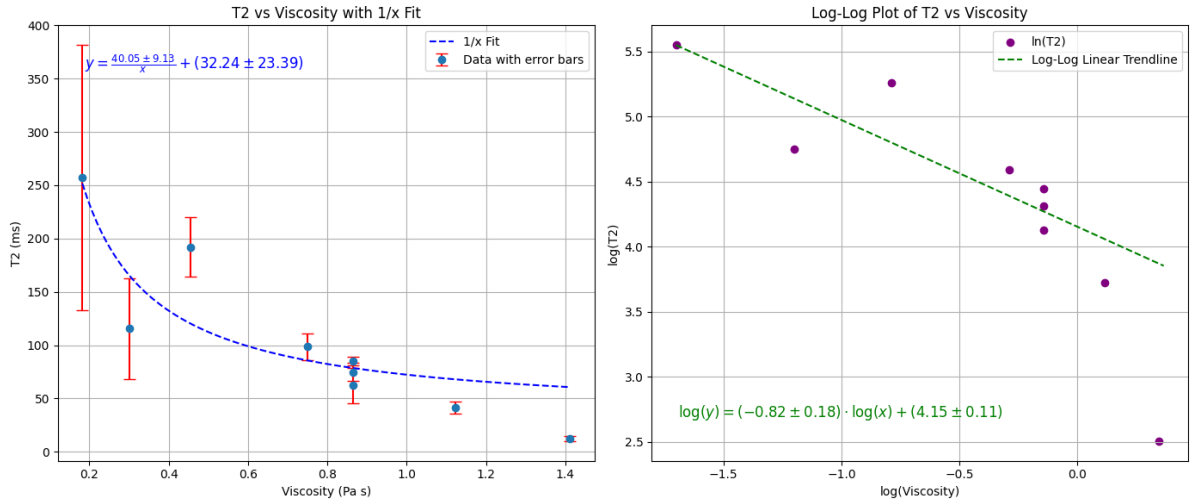

Figure 10: Plot of Spin-Spin Relaxation time for different viscosities of glycerol at 21°C. An inverse relationship between T_2 and concentration is found.

for the log-log graphs are -1.36±0.19 and -0.82±0.18 for T_1 and T_2, respectively. These imply inverse relationships between relaxation times and viscosity.

Example T_1 and T_2 for glycerol and $CuSO_4$ can be seen in table 2.

4.3 Varying Temperature for $CuSO_4$ and Glycerol Samples

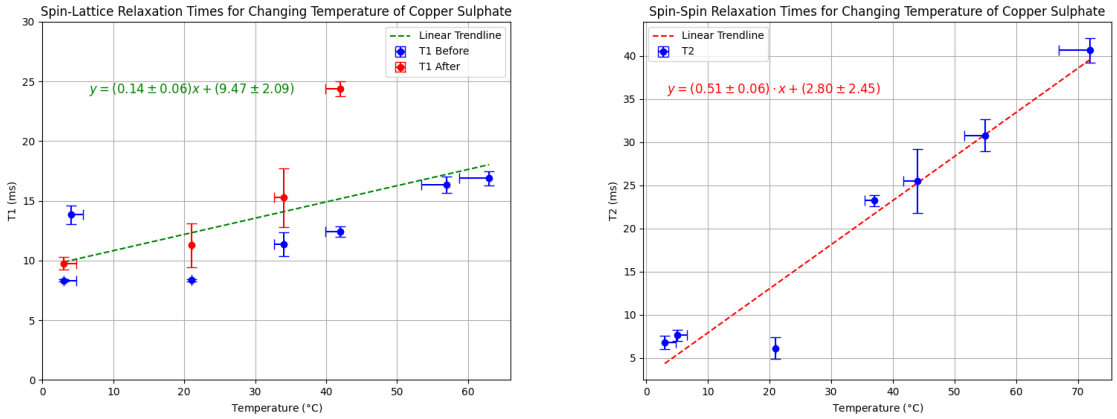

(a) T_1 (b) T_2

Figure 11: Spin-Spin and Spin-Lattice relaxation times for a 6.25% concentration sample of copper sulphate at 21°C. T_1 is seen to be roughly constant with temperature. T_2 is seen to be proportional to temperature.

In addition to the usual errors in the values of T_1 and T_2, the temperature graphs also have a significant error in temperature due to the cooling of the samples inside the magnet.

In figure 11 the T_1 and T_2 values for copper are plotted against temperature for a 6.25% concentration at 21°C. A linear trend can be seen with a shallow gradient of 0.14±0.06 for T_1 and 0.51±0.06 for T_2. Figure 12 plots the same data for an 80% concentration sample of glycerol at 21°C. A linear trend is seen once again; however, this time the

gradients are much more significant. A gradient of 4.19±0.34 is found for T_1 and for T_2 it is found to be 2.94±0.47. There is a much stronger relationship with temperature for glycerol compared to $CuSO_4$.

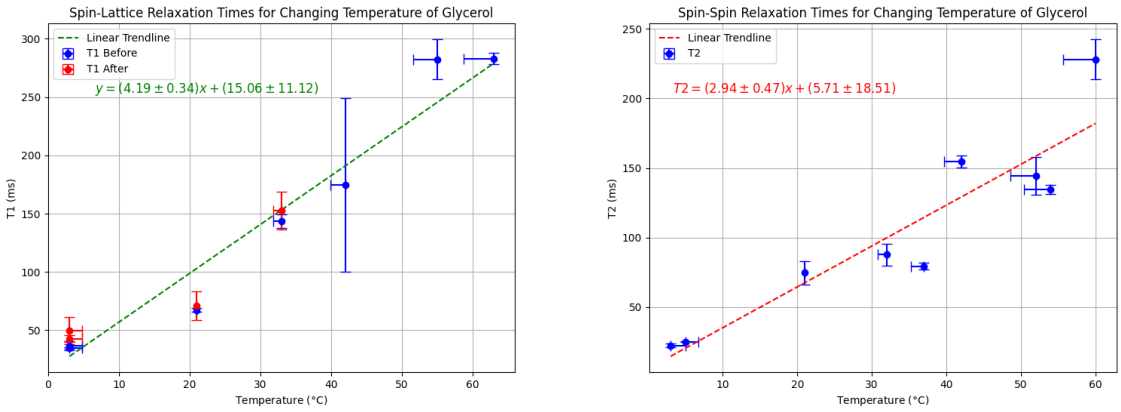

(a) T_1 (b) T_2

Figure 12: Spin-Spin and Spin-Lattice relaxation times for a 6.25% concentration sample of glycerol. Relaxation times are found to be proportional to temperature.

5 Discussion

5.1 Discussion of Experimental Results

5.1.1 Gradient changes in T_1 graphs

The origin for the change in gradient observed in T_1 graphs is unclear. It occurs when the M_z vector reduces through zero and starts pointing in the positive z direction. Interestingly, the T_1 value afterwards is almost always larger than the value before; the values also diverge at lower concentrations.

Further experimentation could be done to determine the cause of the change in T_1, particularly focusing on changes with concentration.

5.1.2 Varying Concentration of Copper Sulphate

It is shown that there is an inverse relationship between the concentration of $CuSO_4$ with T_1 and T_2. This can be explained more easily from the point of view of adding *paramagnetic* $CuSO_4$ to *diamagnetic* H_2O when the *concentration* increases. As discussed in section 2.3 the addition of paramagnetic ions to a sample allows for a quicker relaxation via a dipole-dipole mechanism. Therefore, as the concentration of $CuSO_4$ is increased the relaxation time decreases as more paramagnetic ions are added to the sample.

5.1.3 Varying Viscosity of Glycerol

It is observed that there is a clear inverse relationship between T_1 and viscosity since the gradient of the log-log graph ~ -1 (figure 9). This agrees with the relationship found by Bloembergen[2] in 1948. Furthermore, T_2 follows a similar relationship, which is not unexpected since T_1 and T_2 are closely related. It is observed that $T_2 < T_1$ in almost

all cases, which is to be expected. Samples of higher viscosity have more microscopic interactions since they move around each other slower (reduced tumbling), leading to decreased relaxation times.

5.1.4 Varying Temperature for Copper Sulphate and Glycerol Samples

There is a clear increase in relaxation time for glycerol with increasing temperature. It is known that increasing the temperature of a liquid decreases its viscosity.[8] Therefore, since relaxation time is inversely proportional to viscosity, a positive linear relationship between relaxation time and temperature for a viscous liquid is expected. It is also found that T_1 increases more strongly with temperature than T_2, this is also expected since T_1 increases more strongly with reducing viscosity than T_2 (section 5.1.3).

For $CuSO_4$ there is a small trend of increasing relaxation time with temperature (see figure 11). An increase for $CuSO_4$ is not expected as the relaxation time for $CuSO_4$ is dominated by paramagnetic relaxation, which is not affected by a change in temperature. The small increase could be attributed to slight changes in viscosity, but it is more likely due to random experimental error.

5.2 Discussion of Errors

The results for glycerol have quite significant errors, especially in comparison to the $CuSO_4$. For low viscosities of glycerol, measurements were particularly difficult as the relaxation times were so long, causing equipment limitations to become significant. Additionally, the high viscosity of glycerol made it difficult to pipette accurately.

The errors in temperature measurements were particularly high. Cooling occurred between measurements as a result of having to transfer the samples from the water bath to the magnet as well as the temperature of the magnet being significantly cooler than room temperature. It was impractical to insert temperature probes into the magnet, as this would disrupt the field. Efforts were made to reduce errors by keeping the vials in an insulated container containing hot water; however, it would have been better to reheat the samples between every measurement.

The noise levels seen on the picoscope (see red trace on figure 3) varied significantly day-to-day. Examples of causes of the noise include mains noise and other experiments. This meant readings on certain days had higher errors compared to others. It would have been ideal to record measurements during low noise periods, but this wasn't feasible due to time constraints.

6 Conclusion

This experiment examines the effects of viscosity, changes in temperature, and the addition of paramagnetic ions on the spin-lattice and spin-spin relaxation times in nuclear magnetic resonance (NMR).

Using different concentrations of glycerol, relaxation times are found to be inversely proportional to viscosity, consistent with the results of Bloembergen.[2] Samples of higher viscosity rotate more slowly, leading to increased microscopic interactions and more efficient relaxation.

Relaxation times were found to decrease with the addition of paramagnet $CuSO_4$. This is expected since paramagnetic ions enable more efficient dipole-dipole relaxation mechanisms.

Measuring samples at different temperatures, it is found that increasing the temperature of viscous samples (glycerol) increases the relaxation times. This is expected since increasing temperature decreases viscosity and relaxation times are inversely proportional to viscosity. There is no observed effect on the paramagnetic samples when changing temperature.

7 Further Experiment: Spectroscopy

One of the most prevalent uses of NMR is NMR spectroscopy to identify the composition of chemical samples. This is discussed in detail in section 2.5.

7.1 Equipment & Method

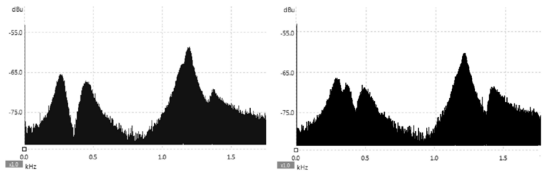

Figure 13: Frequency spectrum of two mystery samples (left: A, right: B)

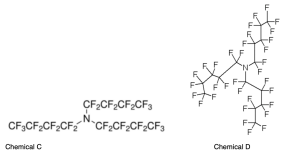

Figure 14: Chemicals C and D

This experiment uses a PS2/B NMR pulsed spectrometer, which has a stronger magnet than the PS1/A as well as additional features required to perform spectroscopy experiments.[9] In this experiment the PS2/B is used to build the spectrum of two mystery compounds. It is known that the mystery compounds are the two compounds given in figure 14, The experiment is conducted to determine which spectrum corresponds to which chemical.

7.2 Results, Discussion and Conclusion

Equation 9 is used to determine the values of the chemical shifts obtained from the spectra in figure 13. The reference sample used is C_6H_5F which is found to have $\nu_{0,\text{ref}}$ =2.2 kHz and the spectrometer frequency ν_{spec} =21.67 MHz. Using this, the chemical shifts are tabulated with reference to C_6H_5F and then converted to the more commonly used chemical shift values with reference compound $CFCl_3$. This is shown in table 3.

Looking at the chemicals in figure 14, both chemicals consist of a nitrogen atom bonded to 3 fluoroalkyl groups. The difference between chemical C and D is that D has one extra CF_2 environment on each of the three branches. The different CF_2 and CF_3 environments produce a peak in the NMR spectra. The three branches are equivalent for both C&D so only one set of peaks will be seen corresponding to the unique environments on the branches. Since chemical D has 5 unique environments and chemical C has 4 unique environments, spectrum A can be assigned to chemical C and spectrum B to chemical D with confidence. It is also the case that the shifts for the larger molecule are higher than

Frequency/kHZ	**Seen in Sample:**	$\delta_{\mathbf{C_6H_5F}}$	$\delta_{\mathbf{CFCl_3}}$
0.259	A	-89.6	-203.1
0.448	A	-80.8	-193.6
1.203	A	-46.0	-159.5
1.379	A	-37.9	-151.4
0.302	B	-87.6	-201.1
0.362	B	-84.8	-198.3
0.491	B	-78.9	-192.4
1.222	B	-45.1	-158.6
1.435	B	-35.3	-148.8

Table 3: Table displaying the chemical shifts from the frequency displays in figure 13

those of the smaller molecule. This is expected as CF_2 groups are electron withdrawing, meaning the fluorines in chemical D are less shielded.

References

[1] I. I. Rabi, J. R. Zacharias, S. Millman, and P. Kusch. A new method of measuring nuclear magnetic moment. *Physics Review Journal*, 1938.

[2] N. Bloembergen, E. M. Purcell, and R. V. Pound. Relaxation effects in nuclear magnetic resonance absorption. *Physics Review Journal*, 1948.

[3] P. J. Hore. *Nuclear Magnetic Resonance (Oxford Chemistry Primers)*. Oxford University Press, 1995.

[4] J. Keeler. *Understanding NMR Spectroscopy*. Wiley-Blackwell, 2010.

[5] R. J. Abraham, J. Fisher, and P. Loftus. *Introduciton to NMR Spectroscopy*. John Wiley & Sons, 1990.

[6] S. Epstein and S. Bohndiek. *Part II NMR Experiment Handout*. 2024.

[7] W. R. Gambill. *How to estimate mixtures viscosities*. Chemical Engineering, 1959.

[8] Christopher J. Seeton. Viscosity-temperature correlation for liquids. *Tribology Letters*, 22, 2006.

[9] TeachSpin. *PS2-A/B/C Instructor's Manual*. 2010.

[10] TeachSpin. *PS1/A Manual*. 2010.

A Appendix - Additional Figures

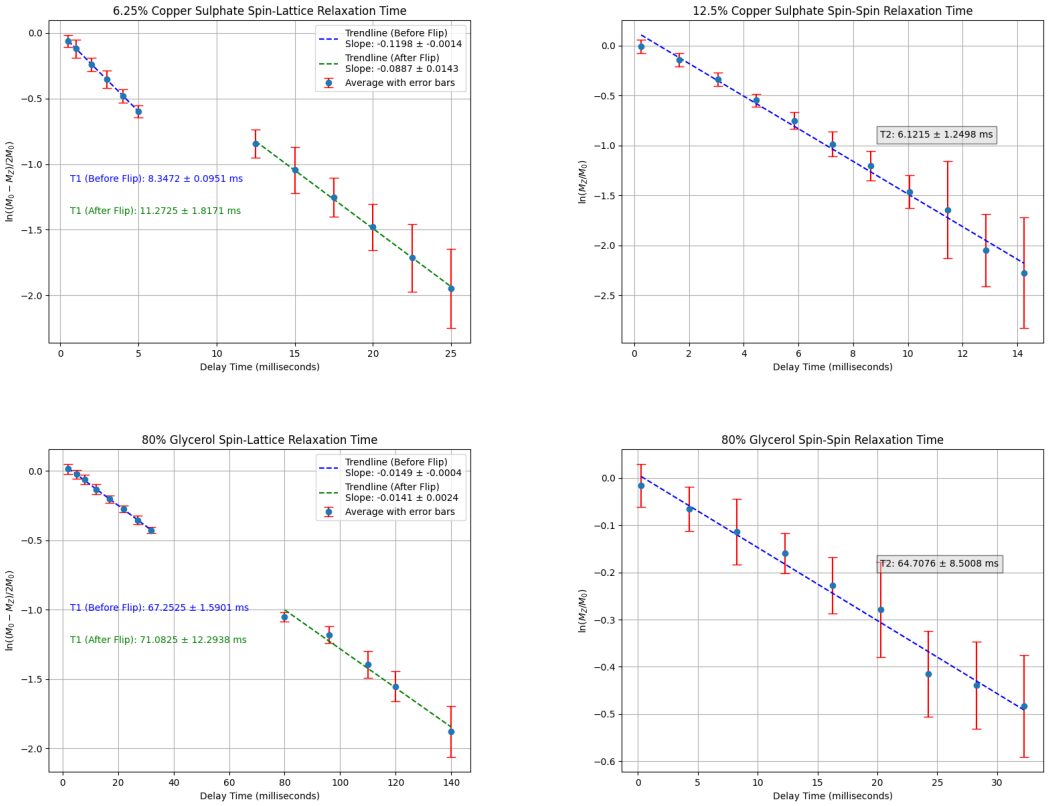

Figure 15: Example T_1 and T_2 graphs where the relevant log is plotted against delay time to determine the relaxation time

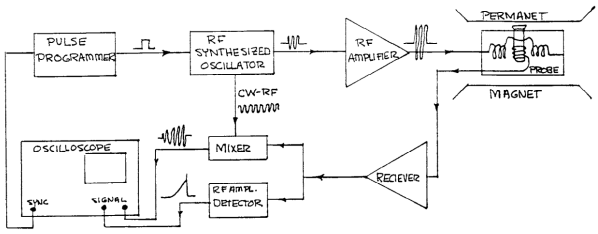

Figure 16: Block diagram of the PS1/A[10]

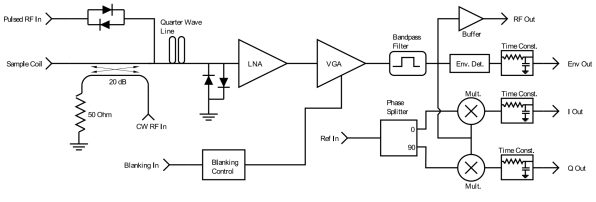

Figure 17: Block diagram of the PS2/B[9]

[Word Count: 2972]